

Temperature dependence of the elastic constants of Ni: reliability of EAM in predicting thermal properties

Majid Karimi[†], Gregory Stapan[†], Theodore Kaplan[‡] and Mark Mostoller[‡]

[†] Physics Department, Indiana University of Pennsylvania, Indiana, PA 15705, USA

[‡] Solid State Division, Oak Ridge National Laboratory, Oak Ridge, TN 37831, USA

Received 16 October 1996, accepted for publication 10 March 1997

Abstract. The temperature dependence of the elastic constants of Ni is calculated using molecular dynamics (MD) simulations in conjunction with the embedded atom method (EAM). The Parrinello–Rahman version of molecular dynamics is employed along with the fluctuation formulae in the $H\sigma N$ and EhN ensembles at various temperatures from 0 K to somewhat below the melting point (experimental value 1725 K). The calculated results for the elastic constants, compressibility, linear coefficient of thermal expansion, specific heat and the melting temperature compare reasonably well to experiment.

1. Introduction

The elastic constants of solids provide valuable information on their mechanical and dynamical properties. In particular, they provide information on the stability and stiffness of materials. Various experimental techniques are available for the measurement of the elastic constants such as ultrasonic wave propagation, neutron scattering and Brillouin scattering, to name a few. Interatomic potentials are usually results of fits to various experimental data at 0 K or room temperature. It is not clear whether simulations performed at other temperatures should still reproduce the experimental data as accurately. Comparison of theoretical and experimental elastic constants and other properties at various temperatures can thus serve as a further measure of the reliability and utility of a potential model.

Andersen [1] has developed a version of molecular dynamics (MD) in which the volume of the computational box can vary but its shape can not. This form of MD can generate the isoenthalpic–isobaric (HPN) ensemble, in which the enthalpy H , the hydrostatic pressure P and the total number of particles N in the system are all constant. The bulk modulus, which is a measure of volume fluctuation, can be determined using the HPN ensemble. The HPN ensemble is appropriate only for the cases where a fixed isotropic pressure is at work and the shape of the computational box does not change. The extension of HPN MD to treat anisotropic external stresses with a variable-shaped computational cell was developed by Parrinello and Rahman [2]. The Parrinello–Rahman extension of HPN MD can generate the isoenthalpic–isostress ensemble ($H\sigma N$), where σ is the stress. An important aspect of $H\sigma N$ MD is that it can be employed in the study of structural phase transformations of solids as functions of temperature and external stress.

There are several theoretical methods for the calculation of elastic constants. In the direct method, one applies a constant stress on the sample and determines the corresponding average strain [2, 3]. From the stress–strain relationship one can then calculate the elastic

constants. The direct method is inconvenient because for the calculation of all the elastic constants several stresses need to be applied at several times. An alternative way to determine the elastic constants is to use the $H\sigma N$ ensemble; Parrinello and Rahman derived a formula in this ensemble that relates average equilibrium strain fluctuations to the elastic constants [2]. There are similar fluctuation formulae in the $H\sigma N$ ensemble for the calculation of the compressibility [2], the specific heat [4] and the linear coefficient of thermal expansion [4]. A shortcoming of $H\sigma N$ MD is the ambiguity about the 'mass' W of the computational cell [2, 3], since the equations of motion depend on this mass. Although it can be proven that the final averaged equilibrium quantities should not depend on W , the coupling between the box and particles inside it is weak and depends on W . Because of the weak coupling it is difficult to equilibrate the box and particles at the same time.

Elastic constants can also be determined using the EhN ensemble [5], where E is the total energy, h is a matrix representing the volume and shape of the computational cell and N is the total number of particles. Although calculation of the elastic constants in the EhN ensemble has been shown to converge faster than the corresponding $H\sigma N$ calculation, it has not been employed more frequently because it requires (a) the second derivatives of the potential, which is not a trivial task for some potential models, and (b) a reference h from a previous $H\sigma N$ MD run.

Finally, the elastic constants of a crystal can be calculated using a Monte Carlo (MC) simulation [6]. The MC method for the calculation of the elastic constants has all the advantages of $H\sigma N$ MD and EhN MD simulations without some of their disadvantages.

Prerequisite to any realistic atomistic computer simulation is a reliable interatomic potential. The embedded atom method (EAM) was originally developed by Daw and Baskes [7] to model the interatomic interactions of face-centred cubic (fcc) metals. Since its development, the EAM has been extended to body-centred cubic (bcc) and hexagonal close-packed (hcp) metals and to semiconductors [8], albeit with somewhat less success for the bcc and tetrahedrally-coordinated materials than for the close-packed metals. The EAM has been applied to many bulk, surface and interface problems. The applications in bulk or bulk-like environments have generally been more successful than corresponding applications for surfaces. This behaviour is expected from the EAM because it is generally fitted to bulk properties. The reliability of the EAM in the bulk and its simple form for use in computer simulations makes it attractive for utilization in the present problem. In our calculations, we have used the EAM functions for Ni developed by Voter and Chen (VC) [9] which were fitted to bulk experimental properties. We chose Ni because it is an fcc metal, and VC's version of the EAM is both easy to use computationally and gives good results for Ni at room temperature.

There has not yet been a comprehensive study of the temperature dependence of various properties of materials using the EAM. In this paper, we study the temperature dependence of several properties of a Ni single crystal using $H\sigma N$ MD and EhN MD. In particular, we calculate the temperature dependence of the elastic constants, compressibility, specific heat and linear thermal expansion coefficient. We also employ a simple model [10] to estimate the melting point. Our results will be compared with the available experimental data. In section 2, highlights of the EAM and MD are described. In section 3, we present our results. A summary and conclusions are given in section 4.

2. Technical approach

In the EAM, the binding energy of atom i is a sum of contributions from the embedding potential and the pair potential,

$$E_i = F_i(\rho_i) + \frac{1}{2} \sum_{j \neq i} \phi_{ij}(r_{ij}) \quad (1a)$$

$$E_{\text{pot}} = \sum_i E_i \quad (1b)$$

where E_i is the energy of atom i , ρ_i is the electronic charge density at site i , F_i is the embedding energy function of atom i and ϕ_{ij} is the pair potential between atoms i and j . ρ_i is approximated by the superposition of atomic charge densities ρ^a . The EAM (VC) functions employed here have a Morse-type pair potential with three free parameters for ϕ_{ij} , and F_i is determined from equation (1a) with E_i approximated with the universal form from the Rose equation of state [11]. The atomic electron density ρ^a has the form presented in [9] with one free parameter. Due to the nature of the fitting process for the embedding function, the lattice constant, cohesive energy and bulk modulus are exact fits to the experimental values. In order to make ρ^a and ϕ_{ij} appropriate for use in computer simulations, they and their first derivatives have been smoothed by the prescription set forth by VC. Four parameters of the EAM functions (three in ϕ and one in ρ^a) are determined by fitting to the bulk properties of a Ni single crystal including the elastic constants C_{ij} and the single vacancy formation energy, and to dimer properties (bond energy and length) [9].

In the MD simulation, Newton's equations of motion are integrated to determine the phase-space trajectories of all atoms in the system using a force function which is derived from the EAM potential in equation (1). The force F_a on atom a is determined from E_{pot} by

$$F_a = -\frac{\partial E_{\text{pot}}}{\partial x_a} \quad (2a)$$

where for the EAM F_a would take the following form,

$$F_a = -\sum_{\substack{b=1 \\ b \neq a}} \left[\frac{\partial F_a}{\partial \rho_a} \frac{\partial \rho_b^{\text{at}}}{\partial r_{ab}} + \frac{\partial F_b}{\partial \rho_b} \frac{\partial \rho_a^{\text{at}}}{\partial r_{ab}} + \frac{\partial \phi_{ab}(r_{ab})}{\partial r_{ab}} \right] \hat{r}_{ab} \quad (2b)$$

where r_{ab} is a vector from atom a to atom b and \hat{r}_{ab} is a unit vector in that direction. Throughout this paper we have adopted the notation of [5]. A prime denotes the derivative with respect to the argument of the function. The microscopic stress tensor for the EAM functions can be determined from the virial theorem and has the following form,

$$P_{ij} = \frac{1}{V} \left[\sum_{a=1}^N \frac{p_{ai} p_{aj}}{m_a} - \sum_{\substack{a,b=1 \\ a < b}} (F'_a \rho_b^{\text{av}} + F'_b \rho_a^{\text{av}} + \phi'_{ab}) \frac{X_{abi} X_{abj}}{r_{ab}} \right] \quad (3)$$

where V is the volume of the computational box, m_a is the mass of atom a , p_{ai} is the i th component of the linear momentum of particle a , X_{abi} is the i th component of the r_{ab} vector and the summation is over all atoms with $a < b$.

In all the simulations, we have used a lattice of 256 atoms arranged in an fcc crystal. The equations of motion are integrated with a fifth order predictor–corrector Nordsieck integration scheme [12], with periodic boundary conditions in three dimensions. We have used time steps which are small enough to conserve energy (enthalpy) in the simulations with good accuracy. The MD simulations were performed for a period of time t_1 using the $T\sigma N$ ensemble (constant temperature), followed by a period t_2 using the $H\sigma N$ ensemble to confirm that thermal equilibrium has been reached, and a subsequent run for a time t_{av} in which statistical averages were calculated.

In the following, we briefly outline the fluctuation formulae that will be employed in the calculations.

2.1. Elastic constants

2.1.1. *HσN ensemble.* The time average of the strain fluctuations is related to the adiabatic compliances η_{ijkl} by [2–4]

$$\langle \varepsilon_{ij} \varepsilon_{kl} \rangle = (k_B T / V_0) \eta_{ijkl} \quad (4)$$

where ε_{ij} is the ij th strain component, T is the temperature, V_0 is the reference volume, and η_{ijkl} is the compliance matrix. The elastic constants matrix C_{ijkl} is the inverse of the compliance matrix. However, the 9×9 η_{ijkl} matrix is singular and does not have a proper inverse. Using the Voigt notation, $11 \rightarrow 1$, $22 \rightarrow 2$, $33 \rightarrow 3$, $23 \rightarrow 4$, $13 \rightarrow 5$, $12 \rightarrow 6$ and, by the prescription set forth in [13], η_{ijkl} is transferred into an equivalent non-singular 6×6 η_{mn} matrix,

$$\eta_{mn} = \begin{cases} 1 \times \eta_{ijkl} & 1 \leq m, n \leq 3 \\ 2 \times \eta_{ijkl} & 1 \leq m \text{ or } n \leq 3, 4 \leq n \text{ or } m \leq 6 \\ 4 \times \eta_{ijkl} & 4 \leq m, n \leq 6. \end{cases}$$

2.1.2. *EhN ensemble.* The fluctuation formula for the calculation of the elastic constants in the *EhN* ensemble was derived in [5],

$$C_{ijklm} = -\frac{V_0}{k_B T} (\langle P_{ij} P_{km} \rangle - \langle P_{ij} \rangle \langle P_{km} \rangle) + \frac{2Nk_B T}{V_0} (\delta_{ik} \delta_{jm} + \delta_{im} \delta_{jk}) + \langle B1_{ijklm} \rangle + \langle B2_{ijklm} \rangle + \langle B3_{ijklm} \rangle. \quad (5)$$

The first term on the right-hand side is called the fluctuation term, the second the temperature correction and the last three are called the Born terms. Pair terms are included in $B1$ and $B2$ while many-body contributions are in $B3$. The Born terms have the following forms for the EAM functions:

$$B1_{ijklm} = \frac{1}{V_0} \sum_{\substack{a,b=1 \\ a < b}} \left[\phi''_{ab} - \frac{\phi'_{ab}}{r_{ab}} \right] \frac{x_{abi} x_{abj} x_{abk} x_{abm}}{r_{ab}^2} \quad (6a)$$

$$B2_{ijklm} = \frac{1}{V_0} \sum_{\substack{a,b=1 \\ a \neq b}} F'_a \left[\rho_{ab}^{av'} - \frac{\rho_b^{av'}}{r_{ab}} \right] \frac{x_{abi} x_{abj} x_{abk} x_{abm}}{r_{ab}^2} \quad (6b)$$

$$B3_{ijklm} = \frac{1}{V_0} \sum_{a=1}^N F''_a g_{aij} g_{akm} \quad (6c)$$

and g_{aij} is given by

$$g_{aij} = \sum_{\substack{b=1 \\ b \neq a}} \frac{\rho_b^{av'} x_{abi} x_{abj}}{r_{ab}}. \quad (6d)$$

It has been shown by Ray [3] that the $T = 0$ elastic constants in the *EhN* ensemble can be determined using the following equation:

$$C_{ijklm} = B1_{ijklm} + B2_{ijklm} + B3_{ijklm}. \quad (7)$$

By comparing equations (5) and (7) one can see that the two are the same if the fluctuation and temperature correction terms are both zero, and the average Born terms are replaced with their values at the $T = 0$ equilibrium lattice positions of the crystal. Equation (7) is determined by taking second derivatives of E_{pot} assuming that the deformation is

homogeneous. The $T = 0$ elastic constants formula is valid for a primitive Bravais lattice with zero strain.

As discussed by Johnson [14], E_{pot} in equation (1) is invariant under the following gauge transformation,

$$F_a(\rho) \rightarrow F_a(\rho) + c_a \rho \quad \phi_{ab} \rightarrow \phi_{ab} - c_a \rho_b^{\text{at}} - c_b \rho_a^{\text{at}} \quad (8)$$

where c_a and c_b are arbitrary constants. Under this transformation $B1 + B2$ as well as $B3$ are invariant. Therefore, if two EAM potentials are related by this gauge transformation, their corresponding $B3$ terms will stay the same. On the other hand, if two different looking EAM potentials generate the same $B3$ at $T = 0$, they can be related by this gauge transformation.

2.2. Compressibility ($H\sigma N$ ensemble)

The fluctuation in volume is related to the compressibility χ by [2]

$$(\langle V^2 \rangle - \langle V \rangle^2) = (\langle V \rangle / \beta) \chi \quad (9)$$

where $\beta = 1/(k_B T)$. The bulk modulus B is the reciprocal of χ .

2.3. Specific heat ($H\sigma N$ ensemble)

The fluctuation in kinetic energy K is related to the specific heat C_σ at constant stress using the following formula [4],

$$\langle K^2 \rangle - \langle K \rangle^2 = 1.5N(k_B T)^2 [1 - 1.5Nk_B / C_\sigma] \quad (10)$$

where N is the total number of particles in the system.

2.4. Linear coefficient of thermal expansion ($H\sigma N$ ensemble)

The linear coefficient of thermal expansion α_{ij} is obtained from fluctuations of the product of kinetic energy K and strain ε_{ij} [4],

$$\langle \varepsilon_{ij} K \rangle - \langle \varepsilon_{ij} \rangle \langle K \rangle = -1.5N(k_B T)^2 \alpha_{ij} / C_\sigma. \quad (11)$$

3. Results

For simulations performed in the $H\sigma N$ ensemble, the system is first brought into equilibrium at zero external pressure and stress at each temperature. MD is run for a period of about 30 ps in the $T\sigma N$ ensemble, after which it continues to run for 150 ps in the $H\sigma N$ ensemble to reach thermal equilibrium. The thermal average properties are determined in a subsequent run of 150 ps. With the time steps chosen ($dt = 0.003$ ps and 0.001 ps for low and high T , respectively), the enthalpy is conserved to one part in 10^4 to 10^5 .

The EhN MD calculation of the elastic constants proceeds as follows. A perfect Ni lattice of 256 atoms is constructed with each atom in its ideal bulk position and a reference $h_0 = \langle h(T) \rangle$ matrix corresponding to the desired temperature from a previous $H\sigma N$ MD run. To reach thermal equilibrium, we perform a short constant temperature run followed by a long constant energy run of about 100 ps; averages are calculated in a subsequent EhN run of 100 ps. We checked the convergence of the elastic constants by increasing the simulation times in steps two and three from 100 ps to 150 ps and did not find any significant change in the results.

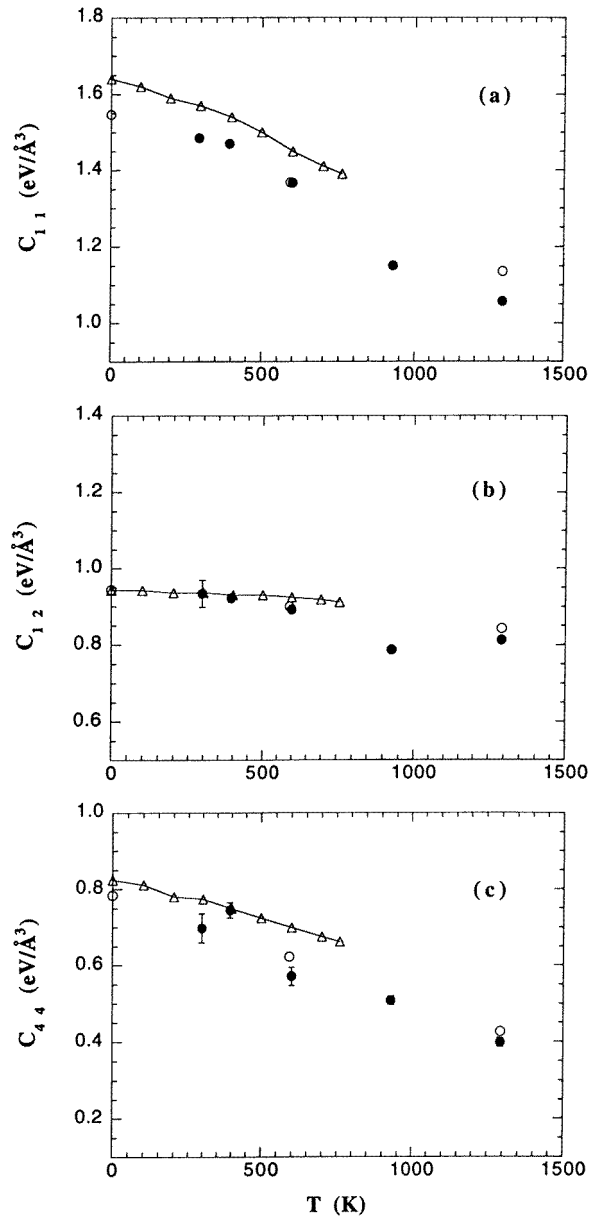


Figure 1. Elastic constants of Ni against temperature: $H\sigma N$ MD, full circles; EhN MD, open circles; experiment [15], open triangles connected with a full curve.

The elastic constants of Ni calculated in these ways are compared with experiment [15] in figure 1. Over the range of 0–760 K for which experimental values are available, the EAM results generally track those measured to within about 10%. It should be noted that VC [9] fitted their potential to room temperature rather than 0 K values for the elastic constants; this accounts in part for the downward shift of the calculated values in figure 1 relative to the experimental results. An estimate of the statistical errors in the calculations can be obtained from the differences between the $H\sigma N$ and EhN results, which are as large as 6.9, 3.6 and 8.3% for C_{11} , C_{12} and C_{44} respectively.

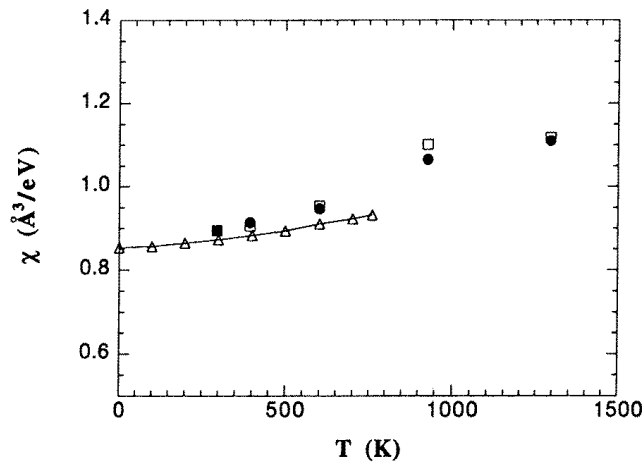


Figure 2. Compressibility of Ni against temperature: *HσN* MD from volume fluctuations (equation (9)), full circles; *HσN* MD from strain fluctuations (equation (4)) and $\chi = 1/B$, open squares; experiment [16], open triangles connected with a full curve.

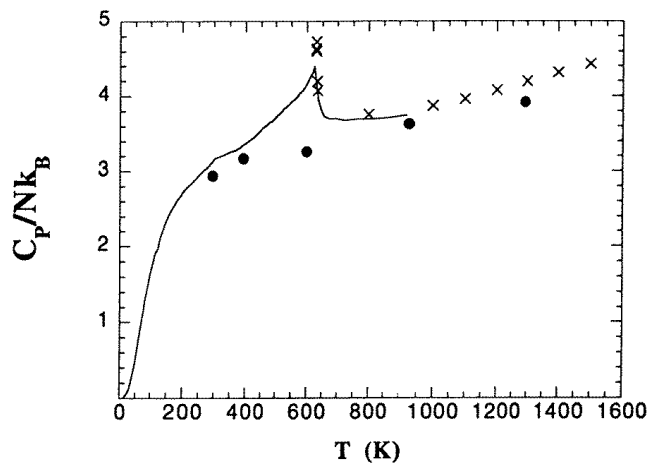


Figure 3. Specific heat of Ni against temperature: *HσN* MD, full circles; experiments [17], full curve and crosses.

The isothermal compressibility χ , the specific heat at constant stress C_σ and the coefficient of linear thermal expansion α have been calculated using the fluctuation formulae in the *HσN* ensemble. Results are shown in figures 2–4 along with the experimental data.

Two sets of calculated results for the compressibility χ are shown in figure 2. One is obtained from the fluctuations in volume in equation (9). The other is determined from the reciprocal of the bulk modulus $\chi = 1/B = 3/(C_{11} + 2C_{12})$, with C_{11} and C_{12} obtained from the strain fluctuations in equation (4). The differences between the two sets of values are small ($< 5\%$), and give another measure of the uncertainties in the calculations. The experimental data is for the bulk modulus [16], which we have converted to compressibility using $\chi = 1/B$. As can be seen in figure 2, the agreement between the simulations and the experiment for χ (recall that the EAM model at $T = 0$ is precisely fitted to B at $T = 0$,

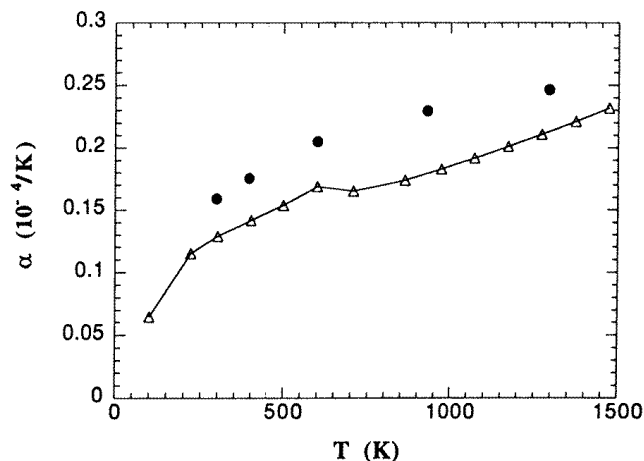


Figure 4. Coefficient of linear thermal expansion of Ni against temperature: *HσN* MD, full circles; experiment [18], open triangles connected with a full curve.

but that VC fitted the room temperature value) is rather good over the range of T covered by experiment, with the difference apparently growing with increasing T .

In figure 3, the calculated specific heat is in good agreement with experiment [17] except in the region around $T \sim 600$ K. Due to the ferromagnetic nature of Ni, which is not included in the EAM calculations, there is a specific heat anomaly around the Curie temperature ($T_c = 631$ K).

Our results for the coefficient of linear thermal expansion are compared to experiment [18] in figure 4. The calculations appear to systematically overstate α by roughly 20%. The experimental results exhibit a small peak at the Curie temperature.

Experimentally, Ni melts at about 1725 K [19]. There are several methods for determining the bulk melting temperature T_M of a crystal. Traditionally, MD simulations are performed on a bulk sample at various temperatures and the cohesive energy is plotted as a function of temperature. At the melting point there is a discontinuity in the cohesive energy. A problem with this approach is that the solid phase can usually be superheated above the melting temperature, and the liquid phase supercooled below T_M . Foiles and Adams [10] determined the thermodynamic melting points of several fcc metals using the free energy, a method which is more involved than that previously described; T_M is obtained as the temperature at which the Gibbs free energies of the solid and liquid become equal.

Another way [10] of determining the melting point of a crystal is to construct a sample and melt half of it to simulate an interface between the liquid and solid. The temperature for which the interface velocity goes to zero is determined as the melting point. We have implemented this approach in samples containing 20 layers along the $z = [001]$ direction with 128 atoms per layer; periodic boundary conditions were imposed in the x and y directions, and free surfaces along z . TVN simulations were performed starting with the first ten layers in the liquid state and the other ten in the crystalline state for various temperatures near the melting point at intervals of $\Delta T = 50$ K. The density profile along z was used to monitor the position of the solid-liquid interface as the simulations proceeded for 10 ps for each value of T . From this procedure, we obtained $T_M = 1630 \pm 50$ K, which is in reasonably good agreement with experiment.

4. Summary and conclusions

We have employed the VC EAM functions for Ni and carried out $H\sigma N$ and EhN MD simulations to calculate the elastic constants, compressibility, specific heat and coefficient of thermal expansion of Ni as a function of temperature. Similar simulations have been performed for Ar by Sprik *et al* [20] using the Lennard-Jones (LJ) potential, for Pd by Wolf *et al* [5] using the EAM in EhN MD, and for the LJ potential in $H\sigma N$ Monte Carlo simulations [6].

Our results for the accuracy and convergence of the elastic constants are consistent with the predictions of [2, 3, 5, 20]. The $H\sigma N$ simulations converge rather slowly at lower temperatures, and more slowly at higher temperatures. The EhN calculations require fewer time steps than the $H\sigma N$ simulations, but the accuracy of the former depends on the accuracy of the cell $h_0 = \langle h(T) \rangle$ determined by a previous run of the latter. It may be more efficient to calculate the elastic constants using the Monte Carlo approach developed in [6]. This converges as fast as the corresponding EhN MD simulations and does not require calculation of the second derivatives of the potential.

Our results for the various physical properties are in reasonable agreement with the corresponding experimental results, and provide another measure of the quantitative limitations of the EAM for bulk fcc metals. The calculated values of C_{11} and C_{44} appear to be systematically low, and those of α systematically high, but they track the experimental data. An estimate of the melting temperature based on the interface velocity technique gave $T_M = 1630 \pm 50$ K, which is in reasonable agreement with the experimental value of 1725 K.

Acknowledgments

We would like to thank M S Daw and S M Foiles for sharing their MD and MS codes with us, and the Pittsburgh Supercomputer Center for Cray time. We are grateful to S Sobolewski for his technical help, and to J R Ray, J Matolyak, H E Donley and J F Cooke for helpful discussions. Support from NASA to one of the authors (MK) is also gratefully acknowledged. This research was sponsored by the Division of Materials Science, US Department of Energy under contract number DE-AC05-96OR22464 with Lockheed Martin Energy Research Corporation.

References

- [1] Andersen H C 1980 *J. Chem. Phys.* **72** 2384
Andersen H C 1981 *J. Appl. Phys.* **52** 7182
- [2] Parrinello M and Rahman A 1982 *J. Chem. Phys.* **76** 2662
- [3] Ray J R 1988 *Comput. Phys. Rep.* **8** 109
- [4] Ray J R 1982 *J. Appl. Phys.* **53** 6441
- [5] Wolf R J, Mansour K A, Lee M W and Ray J R 1992 *Phys. Rev. B* **46** 8027
- [6] Fay P J and Ray J R 1992 *Phys. Rev. A* **46** 4645
- [7] Daw M S and Baskes M I 1985 *Phys. Rev. B* **29** 6443
- [8] Baskes M I 1992 *Phys. Rev. B* **46** 2727
- [9] Voter A F and Chen S P 1987 *Proc. Mater. Res. Soc. Symp.* **82** (Pittsburgh, PA: Materials Research Society) p 175
- [10] Foiles S M and Adams J B 1989 *Phys. Rev. B* **40** 5909
- [11] Rose J H, Smith J R, Guinea F and Ferrante J 1984 *Phys. Rev. B* **29** 2963
- [12] Nordseick A 1962 *Math. Comput.* **16** 22

- [13] Nye J F 1985 *Physical Properties of Crystals: Their Representations by Tensors and Matrices* (Oxford: Oxford Science)
- [14] Johnson R A 1988 *Phys. Rev. B* **37** 3924
- [15] Ledbetter H M and Reed R P 1973 *J. Phys. Chem. Ref. Data* **2** 531
- [16] Simmons G and Wang H 1971 *Single Crystal Elastic Constants and Calculated Aggregate Properties: A Handbook* (Cambridge, MA: MIT)
- [17] Touloukian Y S and Buyco E H 1970 *Specific Heat: Metallic Elements and Alloys* (New York:IFI/Plenum)
- [18] Kollie T G 1977 *Phys. Rev. B* **16** 4872
- [19] Weast R C (ed) 1994 *Handbook of Chemistry and Physics* (Cleveland, OH: CRC)
- [20] Sprik M, Impey R W and Klein M L 1984 *Phys. Rev. B* **29** 4368